

BigC: rapid, scalable and accurate clustering of single-cell RNA-seq data

Nana Wei¹, Yating Nie¹, Hua-Jun Wu^{2, #}, Xiaoqi Zheng^{1, #}

¹ Department of Mathematics, Shanghai Normal University, Shanghai, China.

² Peking University Cancer Hospital and Institute, Beijing, China

Correspondence: hjwu@bjmu.edu.cn; xqzheng@shnu.edu.cn;

ABSTRACT

Identifying cell cluster is a critical step for single-cell transcriptomics study. As the rapid growth of scRNA-seq volumes, an efficient clustering method is required. Although numerous approaches are developed, they are inefficient in computation and poor in scalability. In this work, we introduce BigC, an improved spectral clustering algorithm for efficiently and accurately clustering scRNA-seq data. By employing a sub-matrix representative strategy and scaled exponential similarity kernel function, our method can drastically reduce the clustering time. We demonstrated BigC exhibits better or comparable accuracy than other state-of-the-art methods in 15 benchmark datasets with orders of magnitude lower computational cost, especially for large datasets over million cells. BigC can scale to ultra-large datasets over 10 million cells, while preserving a consistent and accurate count of cell clusters. Furthermore, we demonstrate that BigC can be used to develop a consensus clustering method BigCC, which greatly improves the runtime and scalability of state-of-the-art methods while maintaining accuracy.

Single-cell RNA sequencing (scRNA-seq) has transformed our understanding of development and disease through profiling the whole transcriptome at the cellular level^{1, 2}. It has been widely used to decode cell-to-cell heterogeneity and gain new biological insights, because of its ability to identify and characterize cell types in complex tissues³. Unsupervised clustering approaches have played a central role in determining cell types. However, applying such approaches to large data can be computationally intensive and time-consuming. With several datasets profiling over 1 million cells, the scale of scRNA-seq experiments has rapidly increased in recent years. Therefore, scalability should be considered of equal importance as accuracy in developing new clustering algorithms aiming to address this computational challenge.

Currently, Louvain and Leiden are the most widely used clustering algorithms in scRNA-seq analysis, and have been implemented in numerous tools such as Seurat and Scanpy in the past few years^{4, 5}. They try to partition a graph into coherent and connected subgraphs. Louvain discovers clusters by maximizing modularity, which is

defined as the difference between the number of edges within groups and the expected number of these edges at random multiplied by the scale factors (total number of edges in the graph)⁶. By using a local moving node technique, Leiden is a better variant of Louvain⁷. [HJW1] However, both of them are greedy algorithms and are difficult to obtain the global optimal solution, especially for non-convex optimization problems.

In contrast, spectral clustering can cluster in any shape of the sample space and converge to the global optimal solution if exists^{8,9}. It works by performing an eigen-decomposition of the graph Laplacian and clustering the data on the top m eigenvectors by k-means or other clustering methods. However, traditional spectral clustering methods, require $O(N^2)$ complexity to build a graph and $O(N^3)$ to solve eigenvectors, which is prohibitively expensive for large datasets^{10,11}. In addition, similar to k-means, spectral clustering requires the number of clusters as prior knowledge, which is unavailable for scRNA-seq data analysis. These limitations prevent the application of spectral clustering to scRNA-seq data analysis. However, a sparsity adjacency matrix and sparse eigen-solvers have been recently invented to greatly improve the performance of spectral clustering, which allows its application to scRNA-seq data analysis¹⁰⁻¹².

In this work, we present BigC, a fast and scalable spectral clustering algorithm for ultra-large scRNA-seq data analysis. It employs a sub-matrix representation and scaled exponential similarity kernel to measure the similarity between cells and representatives. BigC can auto determine the number of clusters by using properties of Laplacian eigenvalues or community detection methods on the graph constructed based on representatives. We evaluate our method and three state-of-the-art methods for scRNA-seq clustering including Louvain, Leiden, and k-means, using 31 simulation data with the number of cells ranging from 10 thousand to 40 million. Our method significantly outperforms existing methods in terms of speed, with 5 times faster than the next-fastest methods for ultra-large datasets. Simultaneously, our method can accurately estimate the number of clusters when the input number of cells is larger than 5 million, in such cases, Louvain and Leiden fail to give a reasonable number of clusters. We then collected 15 benchmark datasets (Supplementary Table1) to evaluate the clustering accuracy, and found that our method yields better or comparable clustering performance in terms of accuracy. [HJW2] Due to the advantage of being computationally fast, we then develop a consensus clustering method, BigCC, by integrating the various clustering results obtained by BigC. When compared to the popular consensus clustering algorithm SC3⁵, our method achieves improved clustering accuracy on twelve gold/silver standard datasets, is 100 times faster in general, and can work on large datasets in which SC3 fails to run. BigC and BigCC is an accurate and scalable algorithm that provides a general framework for unsupervised clustering of ultra-large scRNA-seq datasets produced by a growing array of scRNA-seq projects.

Results

Overview of BigC. The workflow of BigC is illustrated in Figure 1. BigC starts with the selection of representatives to reduce the computational complexity (Fig. 1a-b). We first perform k-means clustering on a randomly selected subset of cells. The centroids of the

identified clusters are denoted as the representatives (1000 by default) (Fig. 1b). Next the k-nearest representatives for all cells are identified by the approximated k-nearest neighbor algorithm (Fig. 1c). Then we define the weights between representatives and cells by the scaled exponential similarity kernel, and construct a weighted bipartite graph (Fig. 1d). Finally, we compute the first m eigenvectors of the graph and obtain the final clustering results by k-means by default (Fig. 1e). In the current implementation of BigC, we provide two approaches to determine the number of clusters in a dataset: One is to apply a community detection-based technique on the graph created by representatives, such as the method used by Louvain (Fig. 1f); Another option is to use the characteristics of Laplacian [HJW3] that the number of Laplace zero eigenvalues can be used to determine the graph's connectedness. Based on the distribution of eigenvalues, we use the on the number of near-zero eigenvalues of the Laplacian matrix as the number of clusters.

We demonstrated that our scaled exponentially similar kernels are better suited to scRNA-seq data than traditional Gaussian kernels, which performed very poorly on some datasets (Supplementary Fig. 1). In addition, we studied how the number of representatives and the number of nearest neighbors affected the results in BigC, and discovered that using 1000 representatives and 7 for the number of Knn produced superior results (Supplementary Fig. 4).

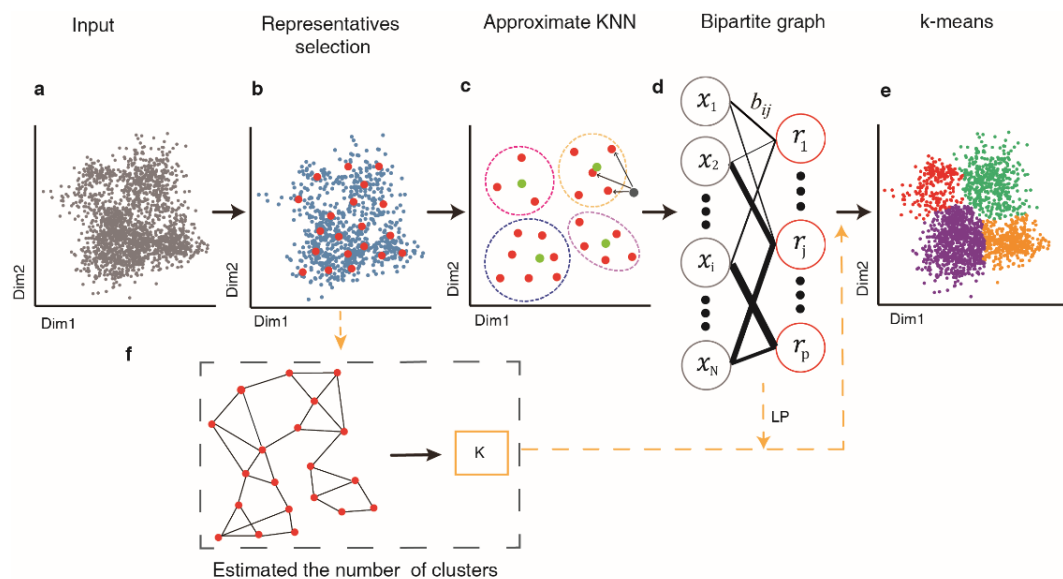


Fig. 1 [HJW4] Framework of BigC for clustering. **a**, BigC takes the matrix in which rows are for cells and columns for features, or the number of clusters m (optional) as input. **b**, The selection of p representatives (red points) based on cells. **c**, The approximate k-nearest neighbors step aims to find the k nearest representatives for each cell by clustering the representatives and using the cluster centers (green points). **d**, A bipartite graph with nodes representing cells and representatives and weights representing Gaussian kernel distances. **e**, Applying the k-means to get final clusters. **f**, BigC estimates the number of the clusters based on graph built by the representatives or eigenvalues of bipartite graph Laplacian (LP).

Performance on simulated ultra-large data. [HJW5] Clustering of ultra-large scRNA-seq datasets is computationally and memory-intensive. We generated a series of scRNA-seq data with an increasing number of cells ranging from 10 thousand to 40 million (see Methods) to test the performance of our and three widely used methods: k-means, Louvain and Leiden (Wolf, et al., 2018). Note that, the true number of clusters is provided to k-means as a comparison. The clustering accuracy is measured using the adjusted Rand Index (ARI) and normalized mutual information (NMI).

We first focused on the performance of different methods as evaluated under computational time. BigC is the fastest on median and large datasets with the number of cells exceeding 50,000. Especially for large datasets with more than 1 million cells, BigC runs 5 times quicker than the second-fastest method k-means. While for small datasets [HJW6] k-means performs better but the variations in runtimes between it and BigC are minor (both below 10 seconds) (Fig. 2a). In contrast, Louvain and Leiden are more computationally intensive than BigC and k-means in datasets of all scales, and the speed is not monotonically increased with the sample size, probably due to the dramatical increase in the number of estimated clusters for large datasets (Fig. 2b). We then investigated the memory consumption of different methods. It appears that BigC and k-means consume the least amount of memory in all datasets. In comparison to Louvain and Leiden, our method only accounts for one-tenth of the Louvain's memory with the sample size over one million (Fig. 2b). In addition, we also evaluated the cluster accuracy of several methods and found that all methods performed similarly with sample sizes fewer than 5 million, however Louvain and Leiden fared poorly with greater than 5 million (Supplementary Fig. 2a).

Next, we sought to investigate the accuracy of our method in deciphering the true number of clusters (K), which are the same ($K = 19$) in simulation data of different sizes (see Methods). Fig. 2b shows the number of clusters identified by three methods, with sample sizes varying from 10 thousand to 40 million. The number of clusters estimated by our method holds out around 18 across datasets. However, Louvain and Leiden failed to give consistent K estimates in large datasets with the number of cells over 5 million (Fig. 2b). The abnormally increased estimates of K can't be easily adjusted by even lowering resolution parameter to 0.0001 (Supplementary Fig. 2b). This suggests that BigC edges in terms of clustering speed significantly while maintaining same or higher accuracy, especially when sample sizes exceed a million.

Additionally, we explored the superiority of our method over the traditional spectral clustering, especially in speed. To do this, we divided the clustering procedure into three parts, including constructing bipartite graph, solving eigen-problem, and final clustering, and compared the runtime of each part between the two methods. Our method significantly reduced runtime on the part of solving eigen-problem, which benefits from the representative selection, making the construction of imbalanced bipartite graph quickly (Supplementary Fig. 2c-d).

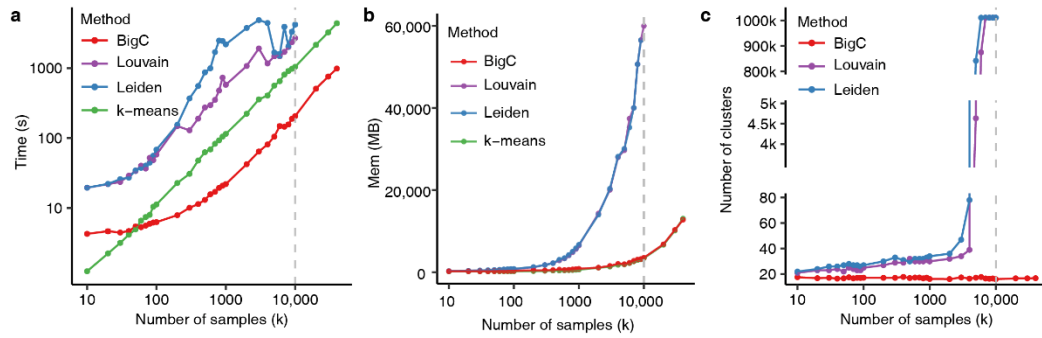


Figure2 The performance of running time and estimated number of clusters across different number of samples from different methods. a, The consuming time in clustering for different methods with the growing number of sample sizes. Note that the number of samples on the x-axis is in thousands here. **b,** The memory consumption of different approaches changes as the sample size grows from 10,000 to 40 million. **c,** The estimated number of clusters for three methods, i.e., BigC, Louvain and Leiden.

BigC fast and accurately clusters large [MOU7] real datasets [HJW8]. To further evaluated the clustering time and accuracy of our method on real datasets, we collected three large ones generated recently, i.e., COVID-19 consists of 1.46 million immune cells isolated from 196 patients; MCA contains 325, 486 cells of the major mouse organs; Mouse brain dataset consists of over 1 million cells from two E18 mice. For each dataset, we performed the clustering methods 10 times to obtain a stable runtime and clustering accuracy.

Our method takes the minimum time on all datasets (Fig. 3a). In COVID-19 dataset at the scale of million cells, our method takes less than one minutes on average to complete clustering, which is 3 times faster than k-means, and 24 times faster than Louvain and Leiden. Simultaneously, BigC exhibits similar clustering accuracy to Louvain and Leiden in general, with higher accuracy in COVID-19, MCA and lower in Mouse brain datasets, respectively (Fig. 3b) [HJW9]. Similar results are obtained by using NMI score (Supplementary Fig. 3c). An example of the clustering results by all methods are demonstrated in UMAP visualization (Fig. 3c-i), in which Reference is obtained by Xie et al.¹³. Under the default parameters, the BigC, Louvain and Leiden show a similar distribution at cells on the left of UMAP distribution (Fig. d-f). Due to Louvain and Leiden have a large number of clusters by default, we modify their resolution to match BigC's (Fig. 3e, f). When the number of clusters is the same, it can be observed that Louvain and Leiden struggle to identify the Interneurons and Neural stem/precursor cells in the lower left corner, which both are labeled as the same cluster, i.e., cluster 3 in Louvain and cluster 5 in Leiden. Likewise, k-means also group them into one (cluster 15) even given the real number of clusters. These findings demonstrate that BigC is an accurately and computationally efficient algorithm for clustering large scRNA-seq datasets.

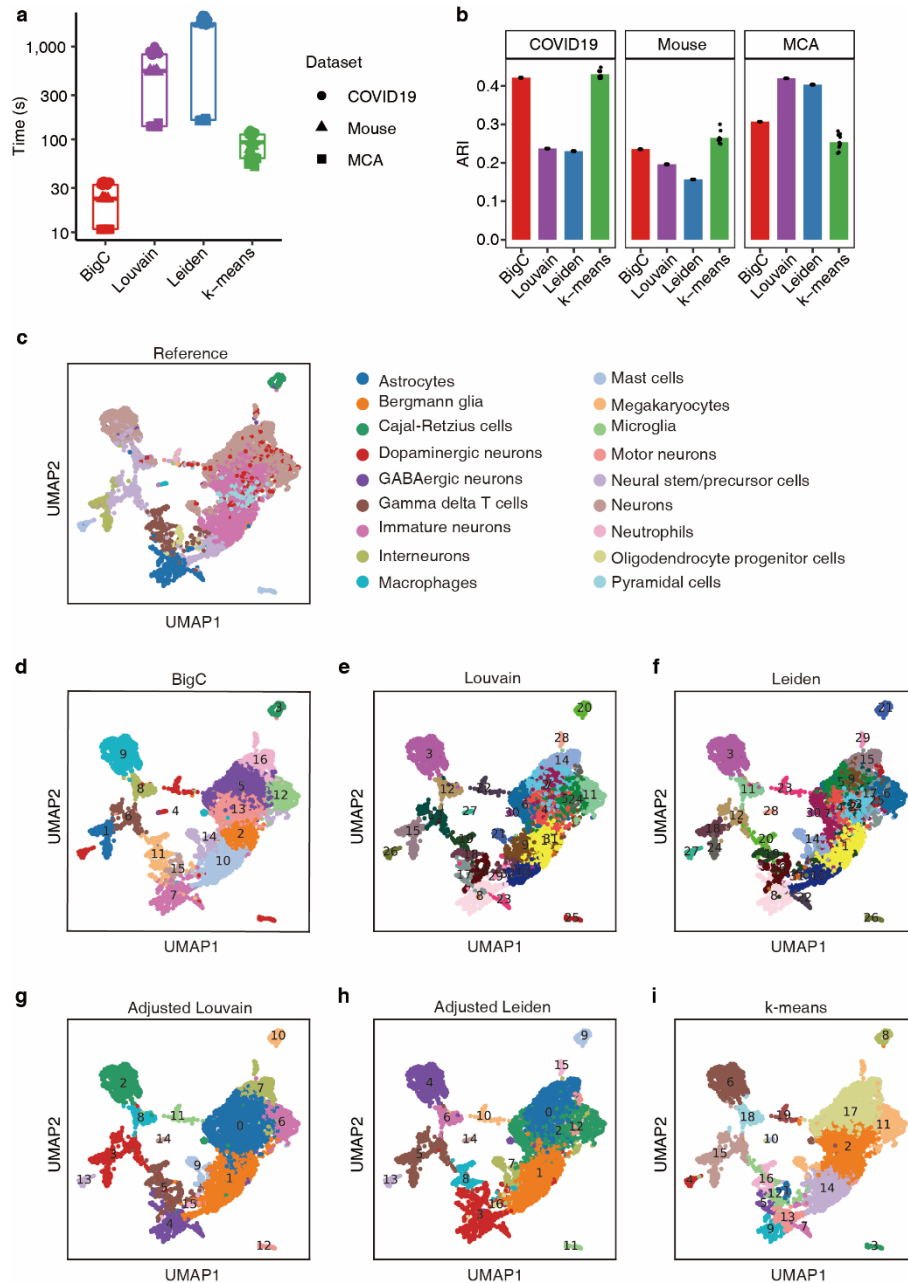


Figure3 [HJW10][魏11] **Performance of different methods on real large datasets.** **a**, The clustering time of different methods. **b**, The ARI of the different methods on three large datasets. **c-i**, Distribution of different method on COVID-19 dataset. The reference represents the ground-truth distribution map, and the labels are annotated by other authors. BigC, Louvain, and Leiden obtained their results using the default parameters of their respective methods. Adjusted Louvain and adjusted Leiden refer to the clustering results at the lower resolution of 0.3. Here k-means is given the true number of clusters.

BigC achieves satisfactory performance on twelve benchmark datasets with known cell type annotations. We next evaluated [MOU12] the different methods on six gold standard and six silver standard datasets introduced by SC3, scDCC and MARS^{5, 14, 15}. Although these datasets are relatively small in size (ranging from 49 to 110,000 cells per set), they have a high-confidence cell type labels, and are widely used to test the

performance of new clustering methods.

As expected, BigC keeps the same fastest running speed as k-means which is 10 times quicker than Louvain and Leiden across datasets (Fig. 4a). In the meanwhile, BigC outperforms Louvain and Leiden in 7 out of 12 datasets (Fig. 4b and c), and is significantly better than them on 4 datasets (Goolam, Biase, Human kidney and Mouse retina). The total ARI of all datasets shows that our method is highly competitive (Fig. 4d). Likewise, similar trends are observed for NMI of different methods (Supplementary Fig. 3). While k-means is comparable to BigC in terms of accuracy, it's quite unstable, especially with Biase data, where the maximum and worst ARI are separated by 0.5. Furthermore, we found that k-means is extremely sensitive to the data preprocessing pipelines (Supplementary Fig. 6). The UMAP visualization of an example dataset depicts the clustering of BigC is more in line with the underlining cell type annotations (Fig. 4e-i). It is worth mentioning that for reference cluster 5, cluster 1 identified by our method can be perfectly matched to it. None of the other approaches are capable of detecting this. Finally, we examined the accuracy of the estimated number of clusters from different methods on these 12 datasets and discovered that our two implementations outperformed Louvain and Leiden (Supplementary Fig. 5). These results demonstrate an appealing advantage of our algorithm in small scRNA-seq datasets.

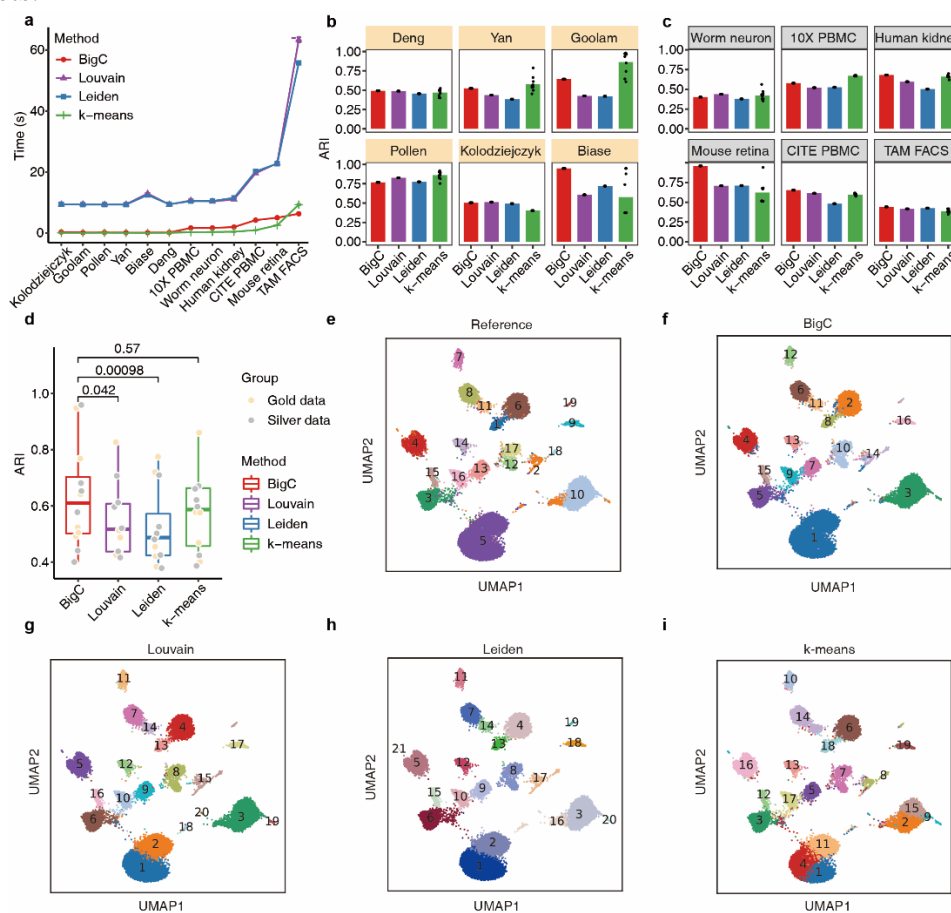


Figure4 Performance of BigC in twelve datasets. a, The running time of clustering of each method on twelve datasets. **b-c,** Accuracy of the different methods, including k-means, Louvain, Leiden,

and BigC, on gold (a) and silver (b) standard datasets. **d**, A boxplot showing the overall ARI of different methods on all datasets. e-i Scatter plots displaying the distribution of clusters identified from different methods. **e-i**, Distribution on Mouse retain data from reference and clustering results from four different methods.

Consensus clustering of BigCC achieves improved clustering on gold/silver standard data. Most of the unsupervised clustering algorithms could yield an inconsistent result due to random initials and parameter settings. To solve this common problem, consensus clustering integrates multiple outputs, generated by different clustering algorithms or the same algorithm with different parameter settings, to produce consensus clusters that are believed to be more robust and accurate⁵. However, consensus clustering method for scRNA-seq data, especially for large-scale ones, is still lacking due to the computational and memory complexity. Here, we developed BigCC, a consensus clustering method to ensemble results from multiple outputs of BigC run by taking advantage of its high running speed. The implementation of the algorithm consists of three steps (Fig. 5a): First, BigC was performed M times with different distance metrics, including Euclidean and cosine, and numbers of clusters estimated by different parameter settings to generate multiple clustering outputs. Second, an unweighted bipartite graph was constructed based on the multiple outputs. Third, the k-means clustering was performed on the graph.

We then evaluate the performance of BigCC on twelve gold/silver standard datasets by comparing it to SC3, a widely used consensus clustering method, and BigC. We compared the times of individual clustering input by BigC and found it performs well with 5 to 10 (Supplementary Figure 7). Therefore, we here set M as 5 for all datasets. It can be found that BigCC is over 100 times faster than SC3 in all datasets (Fig. 5b). More specifically, BigCC completes clustering in an average of 1 second on the gold standard datasets, while SC3 takes more than 100 seconds. Furthermore, SC3 takes over 2 hours for processing some silver datasets which only takes 38 seconds for BigCC to complete. More importantly, BigCC can process large datasets of 27, 499, and 110,832 single cells in 50 seconds, on which SC3 fails to run. With the exception of the time advantage, BigCC exhibits better or equivalent accuracy than BigC in all datasets and significantly outperforms SC3 in five datasets (Biase, Goolam, Worm neuron, Human kidney and CITE PBMC), while marginally better than SC3 on four datasets (Deng, Pollen, Kolodziejczyk and 10X PBMC). These findings indicate that our proposed algorithm is an appealing option for consensus clustering of large scRNA-seq datasets.

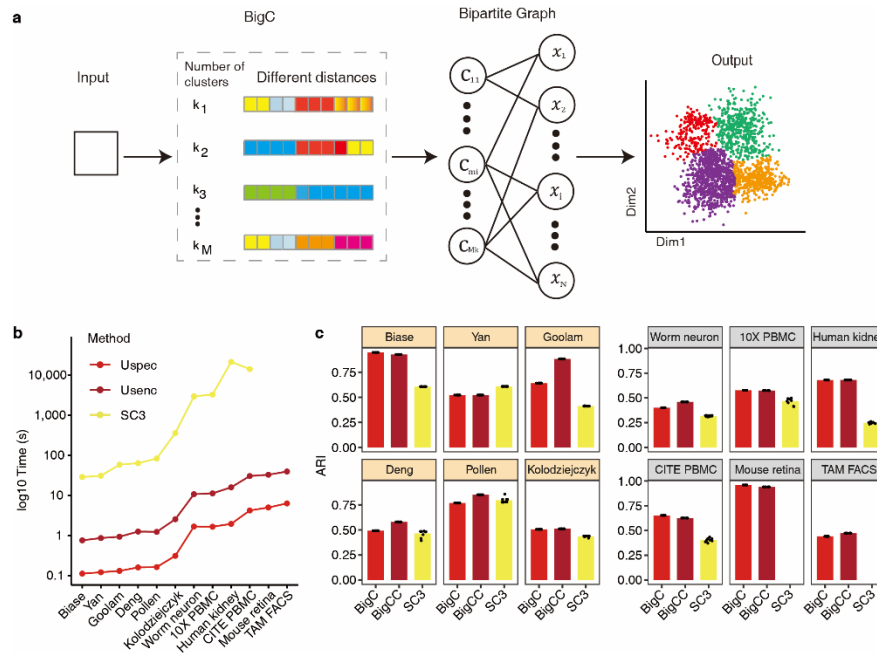


Figure 5 The framework of BigCC and the performance on gold/silver standard datasets. a, BigCC uses a matrix as input, with genes in the columns and cells in the rows, then runs BigC M times to acquire the multiple individual clustering results. The bipartite graph is then constructed, with edges consisting of clusters and cells. Finally, k-means clustering is used to get at a consensus grouping. **b,** The running time of clustering for different methods. **c,** The ARI for three methods on gold/silver standard datasets.

Summary

Identifying cell clusters is a critical step for scRNA-seq data analysis. Effective methods are necessary due to the rapidly expanding volume of scRNA-seq data. In this study, we have presented BigC as a computationally efficient, ultra-scalable and accurate method for the unsupervised clustering of scRNA-seq data. BigC is on average 10 times faster than Louvain and Leiden while exhibiting similar accuracy in 15 benchmark datasets, covering different sequencing technologies with the number of cells ranging from 49 to 1.4 million. BigC can efficiently scale to ultra-large scRNA-seq datasets of more than 10 million cells, which Louvain and Leiden are unable to process. For instance, BigC can complete the clustering of scRNA-seq dataset of 10 million cells within two minutes, which is 6 times faster than k-means, one of the most efficient clustering algorithms. In addition, BigC can reliably and accurately estimate the number of cell clusters independent of sample size, while Louvain and Leiden usually fail to return a reasonable cluster number (Identified > 0.9 million clusters) in datasets of over 5 million cells. This allows BigC to process ultra-large scRNA-seq data generated by single cell consortiums.

Moreover, we have proposed a consensus clustering method BigCC by assembling multiple BigC runs with varied parameter settings. BigCC displays better or equivalent accuracy than BigC and SC3 in 12 benchmark datasets, while processing the data in less than 1% the time taken by SC3. This allows BigCC to cluster cell types with increased precision compared to the other methods, while using substantially less

computation than SC3.

Our framework makes a good balance between accuracy, computational cost and scalability. BigC is an attractive choice for clustering large-scale scRNA-seq atlas, and can also be used for real-time analysis for online applications of scRNA-seq databases. The computational efficiency of BigC makes it an appealing choice for ensemble clustering. The proposed ensemble/consensus clustering algorithm - BigCC- can be used for clustering small and medium sized data, or for sub-clustering tasks. The computational efficiency and scalability of consensus clustering remains a limitation, and provoke further work in the field of single cell data analysis. As the rapid development of droplet-based single cell technologies, our framework can be used to identify cell clusters in other large-scale omics data such as scATAC-seq, CyTOF and image-based spatial data.

However, our method has several limitations, such as the random selection of candidate representatives, which may make finding sparse clusters challenging. We'll look into adjusting some other ways in the future, such as density-based down sampling method to choose candidate representatives, or sub clustering to relieve this problem, which is also a typical method for finding sparse groupings.

Methods

Datasets. Fifteen publicly available datasets, including six gold-standard datasets, six silver-standard datasets and three large datasets, are used to evaluate the clustering accuracy of our method (see Supplementary Table1 for details) ^{1, 16-28}. In six gold-standard datasets, cells are highly confident to be labeled as a specific cell type/stage according to their surface marker. In silver standard datasets, the label of each cell is assigned by computational tools or prior knowledge of the authors. Although widely used to benchmark a newly proposed clustering method ^{5, 14, 29}, these datasets are relatively small in size (from 49 to 110, 000 cells per set), and inadequate to evaluate a new method designed for current throughput. Thus, we also assessed our method on three large datasets, which consist of 1 million cells on average.

Data preprocessing. The preprocessing involves four steps: i) gene/cell filtering; ii) normalization; iii) selection of highly variable gene; iv) dimension reduction by PCA. The parameters of entire pipeline are same for all datasets except for the first step. For six small size gold standard datasets, we adopted a preprocessing strategy of gene filtering similar to SC3 ⁵. In detail, we removed genes that are expressed in less than 10% or more than 90% of the cells by the 'gene filter' function in the Scanpy package (Wolf, et al., 2018). For larger datasets including 10X PBMC, Worm neuron, Human kidney and Mouse retain datasets, we filtered cells with fewer than one gene and retained genes expressed in at least one cell using Scanpy[HJW13]. For mouse brain, we excluded cells with fewer than 200 genes and mitochondrial genes with a UMI greater than 5%. And genes expressed less than 3 cells was removed. For TAM FACS, we retained genes expressed in at least 3 cells and cells with no less than 250 genes and 5000 counts. For MCA, cells with fewer than 100 genes and genes with less than 3 cells were excluded. After filter, raw count matrix was normalized and log transformed to

detect highly variable genes (HVG). Finally, Principal Component Analysis (PCA) was performed on the selected HVGs, and the top 50 PCs were retained for clustering. For COVID-19, we downloaded the processed data provided by the authors [HJW14] to facilitate the comparison.

Note that two optional steps of data preprocessing, i.e., normalization and selection of HVGs, can potentially affect the performance of clustering results^{30, 31}. We thus compared the clustering accuracies of different methods with and without these two steps (Supplementary Figure 6).

Spectral clustering. Spectral clustering is a popular clustering algorithm based on graph theory. Given a graph $G = \{X, E, S\}$, where $X = \{x_1, \dots, x_N\}$ is a set of data points, E is a set of edges and $S = [S_{ij}]_{i,j=1,2,\dots,N}$ is a weighted adjacency matrix or similarity matrix, spectral clustering aims to divide the graph into some disjoint subgraphs in which the weights of edges within-group are as high as possible while those between two groups are as low as possible. A typical spectral clustering algorithm consists of the following main steps: 1) construction of an adjacency matrix S for data points based on certain distance measurements (e.g., Euclidean, cosine, etc.); 2) Computing the Laplacian matrix, i.e., $L = D - S$, where D is the degree matrix of the graph, which is a diagonal matrix with diagonal elements equal to the row sums of S ; 3) Calculating the eigenvectors corresponding to the m smallest eigenvalues of the (normalized) Laplacian, then arrange them in a matrix V by columns; 4) Clustering the row-normalized V into m groups using conventional clustering algorithms, such as k-means and hierarchical clustering. Until now, spectral clustering has several variant versions according to different forms of the Laplacian matrix⁸. Among them, the Normalized cut (Ncut) method is the most widely adopted⁹.

BigC. Our BigC method tailors conventional spectral clustering for large-scale scRNA-seq data from the following two aspects. Firstly, a submatrix strategy by selecting representatives from all samples is introduced to avoid the computation of dense adjacency matrices and determine the weight of graph using a scaled exponential similarity kernel function. Secondly, to estimate the number of clusters, we designed two approaches based on the selected representatives. In summary, our method mainly contains four parts. 1) selection of representatives; 2) estimation of cluster number. 3) approximative k nearest neighbors; 4) bipartite graph partitioning. Among them, the step of selection of representatives to generate a sub matrix of cell-by-representative substituting the dense similarity matrix is critical for significantly improving clustering speed and storage.

Selection of representatives. Given a dataset $X = \{x_i\}_{i=1,\dots,N}$, where $x_i \in \mathcal{R}^f$ represents a cell with f features. We used p (default by 1000) representatives to avoid the computation of the dense similarity matrix. The idea behind this step is to use a set of landmark points to approximately represent the structure of the data. In detail, we first randomly selected p' candidate cells from all cells such that $p < p' \ll N$, then clustered candidate cells into p clusters by the k-means clustering. The final

representatives are the centers of p clusters, denote as $r = \{r_1, r_2, \dots, r_p\}$.

Estimation of cluster number. The number of clusters should be specified for conventional spectral clustering algorithms. However, in most cases, the true number of cell types are not available. Inspired by the community detection algorithms that can infer number of clusters using a resolution parameter, we here utilize the selected representatives to approximately estimate the number of clusters by a graph-based method. In current version of BigC, we implemented two approaches for estimating the number of clusters. One approach is based on the number of near-zero eigenvalues of the Laplacian matrix, which is proved to be associated with the number of connected components of the graph. In detail, the bipartite graph Laplacian matrix's eigenvalues are ordered in ascending order first. The data is then divided into 100 bins, and the predicted number of clusters is calculated by counting the frequencies of the bins to the left of the g -th largest gap. The other is the community detection based (Louvain) approach, but implemented on p representatives rather than all cells. take the number close to 0 as the number of clusters.

Approximative k nearest neighbors. Given p representatives, we aimed to construct an $N \times p$ similarity matrix S between all cells and p representatives. However, this step is still computational and memory intensive for ultra-large datasets. To alleviate this problem, we used a modified approximative k nearest neighbors (MAKNN) algorithm to improve the effectiveness. Basically, instead of building a dense adjacency matrix that is computational infeasible for large datasets, this method aims to approximatively find k nearest representatives for each cell to build a sparse adjacency matrix. In brief, we first approximatively find the representative closest to the cell x_i , and then use the representative's neighbors as the cell's neighbors [HJW15](see more details for Supplementary material).[魏16]

We next use a scaled exponential similarity kernel to determine the weight of cells and representatives, and obtain a $N \times p$ adjacency matrix B with each row only keeping k nonzero elements as

$$B = [b_{ij}], i = 1, 2, \dots, N, j = 1, 2, \dots, p,$$

$$b_{ij} = \begin{cases} \exp\left(-\frac{\|x_i - r_j\|^2}{2\sigma_i^2}\right), & \text{if } r_j \in N_k(x_i), \\ 0, & \text{otherwise,} \end{cases}$$

where $N_k(x_i)$ represents the k nearest representatives of cell x_i , and σ_i is the average of the distances between cell x_i and its k nearest representatives. [MOU17]

Bipartite graph partitioning. Putting all cells and representatives together, we constructed a bipartite graph $G_b = \{X, r, W\}$, where W is a weighted adjacency matrix of $(N + p) \times (N + p)$, denoted as:

$$W = \begin{bmatrix} 0 & B \\ B' & 0 \end{bmatrix}.$$

Then the spectral clustering is used for partition of the graph by solving the generalized eigen-problem:

$$Lf = \gamma Df, \quad (1)$$

where $L = D - W$ is the Laplacian matrix, $D = \begin{bmatrix} D_X & 0 \\ 0 & D_p \end{bmatrix}$ is the degree matrix of the graph G_b .

For large datasets which number of cells is far greater than the number of representatives, we employed an efficient method called transfer cuts³², by taking advantage of the unbalance of bipartite graph G_b

$$L_p z = \lambda D_p z, \quad (2)$$

where $L_p = D_p - W_p$, $W_p = B'D_N^{-1}B$. Note that $D_p = \text{diag}(B'\mathbf{1}_p) = \text{diag}(W_p\mathbf{1}_p)$.

That means L_p is actually the Laplacian matrix of the graph $G_p = \{r, W_p\}$.

Li et al proved that the solution of eigen-problem (1) on graph G_p the solution of the eigen-problem (2) on bipartite graph G_b is equivalent³². Let $\{(\lambda_i, z_i)\}_{i=1}^m$ be the first m eigenpairs of (2), where $0 = \lambda_1 < \lambda_2 < \dots < \lambda_m < 1$, and $\{(\gamma_i, f_i)\}_{i=1}^m$ be the first m eigenpairs of (1), where $0 \leq \gamma_i < 1$. According to³² we have the following conclusions

$$\begin{aligned} \gamma_i(2 - \gamma_i) &= \lambda_i, \\ f_i &= \begin{bmatrix} t_i \\ z_i \end{bmatrix}, \end{aligned}$$

where $t_i = \frac{1}{1-\gamma_i} P z_i$, and $P = D_N^{-1}B$ is the associated transition probability matrix from cells to representatives.

After normalizing the matrix $T = [t_1, \dots, t_m]_{N \times m}$ to the unit length, k-means is applied to the rows of normalized matrix to obtain the clustering result. Note that k-means here can be also replaced by other clustering algorithms such as DBSCAN or hierarchical clustering.

BigCC. Taking advantage of BigC's low computational cost, we proposed a consensus clustering method BigCC, which integrates multiple clustering results by BigC to get more consistent and accurate clusters. The implementation of the method is as follows. Firstly, h different base clustering results are obtained by BigC, by varying the selection of representatives, the number of clusters, and the distance metrics between cells (Euclidean or cosine). Denoted all clusters in h base clustering results as $C = \{c_1^1, \dots, c_1^{h_1}, c_2^1, \dots, c_2^{h_2}, \dots, c_h^1, \dots, c_h^{h_m}\}$, where h_i is the number of clusters in the i -th

clustering result and c_i^j is the j -th cluster of the base clustering c_i . Then, a bipartite graph $G_{xc} = \{X, C, \tilde{W}\}$ is constructed according to the cell and these clustering results, in which the nodes are the cells and clusters and \tilde{W} is an $(N + h_c) \times (N + h_c)$ affinity matrix indicating whether the cell belongs to a cluster.

Similar to the BigC section, we next solve the eigenvalue of G_{xc} by transfer cuts (see Supplementary material for more detail). Then k-means is applied to the top m eigenvectors to generate the final clustering result.

Clustering metrics. [MOU18] We compared the clustering accuracy for different methods using the adjusted rand index (ARI) and normalized mutual information (NMI), which are widely used methods for evaluating the clustering performance with true labels known. ARI can be formulated as

$$ARI = \frac{\sum_{i,j} \binom{n_{ij}}{2} - [\sum_i \binom{n_i}{2} \sum_j \binom{n_j}{2}] / \binom{n}{2}}{\frac{1}{2} [\sum_i \binom{n_i}{2} + \sum_j \binom{n_j}{2}] - [\sum_i \binom{n_i}{2} \sum_j \binom{n_j}{2}] / \binom{n}{2}},$$

where n is the total number of cells, and n_{ij} represents the number of overlap cells that are shared by predict cluster i and true label j , n_i and n_j are the number of cells in predict cluster i and true label j , respectively. NMI can be computed as

$$NMI = \frac{\sum_{i,j} p_{ij} \log \frac{p_{ij}}{p_i p_j}}{(-\sum_i p_i \log p_i - \sum_j p_j \log p_j) / 2}$$

where $p_{ij} = \frac{n_{ij}}{n}$, $p_i = \frac{n_i}{n}$ and $p_j = \frac{n_j}{n}$. A higher value of ARI and NMI indicates better clustering result.

Data available

The dataset in this study are available: Biase, Yan, Goolam, Deng, Pollen and kolodziejczyk (<https://hemberg-lab.github.io/scRNA.seq.datasets/>), Worm neuron, 10X PBMC, CITE PBMC, and Mouse retain and Human kidney (<https://github.com/ttgump/scDCC/tree/master/data>), TAM FACS (https://figshare.com/projects/Tabula_Muris_Senis/64982), MCA (https://figshare.com/articles/dataset/MCA_DGE_Data/5435866), and COVID19 (<https://drive.google.com/file/d/1IwWcn4WYKgNbZ4DpNweM2cKx1x1hbM0/view>).

Code available

Python implementations of BigC are available on GitHub (<https://github.com/nanawei11/BigC>).

References

1. Kolodziejczyk, A.A., Kim, J.K., Svensson, V., Marioni, J.C. & Teichmann, S.A. The technology and biology of single-cell RNA sequencing. *J Molecular cell* **58**, 610-620 (2015).
2. Ziegenhain, C. et al. Comparative analysis of single-cell RNA sequencing methods. *J Molecular cell* **65**, 631-643. e634 (2017).
3. Wang, D. & Bodovitz, S. Single cell analysis: the new frontier in 'omics'. *J Trends in biotechnology* **28**, 281-290 (2010).
4. Duò, A., Robinson, M.D. & Soneson, C. A systematic performance evaluation of clustering methods for single-cell RNA-seq data. *J FResearch* **7** (2018).
5. Kiselev, V.Y. et al. SC3: consensus clustering of single-cell RNA-seq data. *J Nature methods* **14**, 483-486 (2017).

6. Blondel, V.D., Guillaume, J.-L., Lambiotte, R., Lefebvre, E. & experiment Fast unfolding of communities in large networks. *J Journal of statistical mechanics: theory* **2008**, P10008 (2008).
7. Traag, V.A., Waltman, L. & Van Eck, N.J. From Louvain to Leiden: guaranteeing well-connected communities. *J Scientific reports* **9**, 1-12 (2019).
8. Von Luxburg, U. A tutorial on spectral clustering. *J Statistics computing* **17**, 395-416 (2007).
9. Shi, J. & Malik, J. Normalized cuts and image segmentation. *J IEEE Transactions on pattern analysis machine intelligence* **22**, 888-905 (2000).
10. Dhillon, I.S. in Proceedings of the seventh ACM SIGKDD international conference on Knowledge discovery and data mining 269-274 (2001).
11. Huang, D. et al. Ultra-scalable spectral clustering and ensemble clustering. *J IEEE Transactions on Knowledge* **32**, 1212-1226 (2019).
12. Chen, X. & Cai, D. in Twenty-fifth AAAI conference on artificial intelligence (2011).
13. Xie, K., Huang, Y., Zeng, F., Liu, Z. & Chen, T. scAIDE: clustering of large-scale single-cell RNA-seq data reveals putative and rare cell types. *J NAR genomics bioinformatics* **2**, lqaa082 (2020).
14. Brbić, M. et al. MARS: discovering novel cell types across heterogeneous single-cell experiments. *Nature methods* **17**, 1200-1206 (2020).
15. Tian, T., Wan, J., Song, Q. & Wei, Z. Clustering single-cell RNA-seq data with a model-based deep learning approach. *Nature Machine Intelligence* **1**, 191-198 (2019).
16. Biase, F.H., Cao, X. & Zhong, S. Cell fate inclination within 2-cell and 4-cell mouse embryos revealed by single-cell RNA sequencing. *J Genome research* **24**, 1787-1796 (2014).
17. Deng, Q., Ramsköld, D., Reinis, B. & Sandberg, R. Single-cell RNA-seq reveals dynamic, random monoallelic gene expression in mammalian cells. *J Science* **343**, 193-196 (2014).
18. Patel, A.P. et al. Single-cell RNA-seq highlights intratumoral heterogeneity in primary glioblastoma. *Science* **344**, 1396-1401 (2014).
19. Pollen, A.A. et al. Low-coverage single-cell mRNA sequencing reveals cellular heterogeneity and activated signaling pathways in developing cerebral cortex. *J Nature biotechnology* **32**, 1053-1058 (2014).
20. Goolam, M. et al. Heterogeneity in Oct4 and Sox2 targets biases cell fate in 4-cell mouse embryos. *J Cell* **165**, 61-74 (2016).
21. Zheng, G.X.Y. et al. Massively parallel digital transcriptional profiling of single cells. *Nature Communications* **8**, 14049 (2017).
22. Han, X. et al. Mapping the mouse cell atlas by microwell-seq. *J Cell* **172**, 1091-1107. e1017 (2018).
23. Innes, B.T. & Bader, G.D. scClustViz—Single-cell RNAseq cluster assessment and visualization. *F1000Research* **7** (2018).
24. Young, M.D. et al. Single-cell transcriptomes from human kidneys reveal the cellular identity of renal tumors. *Science* **361**, 594-599 (2018).
25. Ren, X. et al. COVID-19 immune features revealed by a large-scale single-cell transcriptome atlas. *J Cell* **184**, 1895-1913. e1819 (2021).
26. Shekhar, K. et al. Comprehensive Classification of Retinal Bipolar Neurons by Single-Cell Transcriptomics. *Cell* **166**, 1308-1323.e1330 (2016).
27. Mimitou, E.P. et al. Multiplexed detection of proteins, transcriptomes, clonotypes and

- CRISPR perturbations in single cells. *J Nature methods* **16**, 409-412 (2019).
28. Cao, J. et al. Comprehensive single-cell transcriptional profiling of a multicellular organism. *Science* **357**, 661-667 (2017).
 29. Tian, T., Zhang, J., Lin, X., Wei, Z. & Hakonarson, H. Model-based deep embedding for constrained clustering analysis of single cell RNA-seq data. *Nature Communications* **12**, 1873 (2021).
 30. Tian, L. et al. Benchmarking single cell RNA-sequencing analysis pipelines using mixture control experiments. *Nature methods* **16**, 479-487 (2019).
 31. Germain, P.-L., Sonrel, A. & Robinson, M.D. pipeComp, a general framework for the evaluation of computational pipelines, reveals performant single cell RNA-seq preprocessing tools. *Genome biology* **21**, 1-28 (2020).
 32. Li, Z., Wu, X.-M. & Chang, S.-F. in 2012 IEEE conference on computer vision and pattern recognition 789-796 (IEEE, 2012).

Supplementary Files

Supplementary table1

Dataset	Protocols	#Cells	#Genes	K			Source
				Refere nce	Louvain	BigC	
Biase	SMART-seq	49	3922	3	3	3	Biase, et al. [1] GSE57249
Yan	TruSeq DNA	90	2903	7	3	3	Yan, et al., 2013 [2] GSE36552
Goolam	Smart-Seq2	124	3212	5	3	5	Goolam, et al. E-MTAB-3321
Deng	SMART-seq	268	3028	10	6	9	Deng, et al. GSE46719
Pollen	SMART-seq	301	3942	11	8	9	Pollen, et al. https://scrnaseq-public-datasets.s3.amazonaws.com/scater-objects/pollen.rds
kolodziejczyk	SMART-seq	704	3212	3	6	7	KolodziejczykESData function of the R package scRNAseq.
Worm neuron	sci-RNA-seq	4186	1525	10	34	28	https://atlas.gs.washington.edu/worm-rna/docs/
CITE PBMC	CITE-seq	3,762	255	15	14	15	https://github.com/ttgump/scDCC/tree/master/data
10X PBMC	10X Genomics	4,217	1,285	8	13	12	Zheng, et al. https://github.com/ttgump/scDCC/tree/master/data

Human kidney	10X Genomics	5685	5707	11	26	17	Young, et al. https://github.com/xuebalia/scziDesk/tree/master/dataset/Young
Mouse retina	Drop-seq	27499	1639	19	20	16	Shekhar, et, al. GSE81905
TAM FACS	Smart-seq2	110823	2846	23	49	25	https://figshare.com/articles/dataset/tms_gene_data_rv1/12827615
MCA	Microwell-seq	325486	2940	47	52	32	Han, et al. https://figshare.com/articles/dataset/MCA_DGE_Data/5435866
Mouse brain	10X Genomics	1011462	1376	19	28	16	https://support.10xgenomics.com/single-cell-gene-expression/datasets/1.3.0/1M_neurons
COVID-19	10x Genomics	1462702	27943	12/64	45	14	Ren, et al. https://drive.google.com/file/d/1IwWcn4WYKgNbZ4DpNweM2cKxlx1hbM0/view

Estimation of number of clusters by eigenvector

The number of zero eigenvalues of the Laplacian matrix can indicate the graph's connectedness, which is an important property of the graph Laplacian matrix. We present a method for estimating the number of clusters from the distribution of eigenvalues based on this inspiration. To begin, transform the eigenvalues to the power of 10, 000, mostly to increase the gap between the values. The eigenvalues are then separated into 100 bins. Find the value corresponding to the largest p_{th} gap position based on the gap value between each bin, denoted as g_p , and count all the eigenvalues smaller than the right value of g_p , that is, the estimated number of clusters. Note that different p is selected here (default by 4), and the estimated number of clusters is different.

Approximative k nearest neighbor

Approximate k nearest neighbor aims to find the k nearest representatives to the sample. The general practice calculates the distances between all cells and p representatives, and finds the closest k representatives. This is, however, computationally and storage-wise infeasible. Therefore, an approximate knn algorithm is introduced here. Taking a cell x_i as an example. Firstly, p representatives are classified into t clusters using k-means, denoted as c_1, c_2, \dots, c_t . Then, based on its Euclidean distance from the cluster centers, cell x_i is then categorized into the closest cluster c_j^i . Thirdly, find the nearest representative of x_i by only calculating the

Euclidean distance between x_i and the representatives in c_j^i , denoted as p_i . Fourthly, apply k-nearest neighbor to p representatives to obtain the k' nearest neighbors of each

representative such that $k < k'$. Fifthly, find the k nearest representatives for x_i by computing the distance between x_i and the k' nearest representatives of p_i . We only need to calculate the k' nearest neighbors of p representations in this approach. Find the neighbor representatives of cell among the representative's neighbors.

The eigen-problem in UFAESC

To get the consensus clustering result, we construct a bipartite $G_{xc} = \{X, C, \tilde{W}\}$, in which the nodes are cells and clusters and \tilde{W} is an affinity matrix. There is no connection inside cells or clusters, and an edge only occurs between the cell and the clusters to which the cell belongs in the graph. \tilde{W} can be represented as:

$$\tilde{W} = \begin{bmatrix} 0 & \tilde{E} \\ \tilde{E}' & 0 \end{bmatrix},$$

where \tilde{E} is a $N \times h_c$ matrix with the following form and h_c is the sum of the number of clusters from all individual clustering results, i.e., $h_c = \sum_{i=1}^m h_i$.

$$\tilde{E}_{ij} = \begin{cases} 1, & x_i \in c_j \\ 0, & \text{otherwise} \end{cases},$$

Then the goal is solving the generalized eigen-problem to obtain the top m eigenvectors:

$$\tilde{L}\tilde{f} = \tilde{\gamma}\tilde{D}\tilde{f}, \quad (2)$$

where $\tilde{L} = \tilde{D} - \tilde{E}$ is the Laplacian matrix of G_{xc} , and \tilde{D} is the degree matrix.

It is obvious that each cell only connects m the clusters. That means each row of \tilde{W} only has m nonzero elements. In other words, the graph is unbalanced, so it can be efficiently solved by the transfer cut algorithm. The eigen-problem of (1) is transferred to the solution of eigen-problem of $G_c = \{C, E_c\}$, which refers to the following problem,

$$L_c\tilde{z} = \tilde{\lambda}D_c\tilde{z}, \quad (2)$$

where $E_c = \tilde{E}'\tilde{D}\tilde{E}$ is the adjacency matrix. $D_c = \text{diag}(E_c\mathbf{1}_N)$ and $L_c = D_c - E_c$ represent the degree matrix and the Laplacian matrix of G_c , respectively.

Let $\{(\tilde{\lambda}_i, \tilde{z}_i)\}_{i=1}^m$ be the first m eigenvalues and eigenvectors of (2), where

$0 = \tilde{\lambda}_1 < \tilde{\lambda}_2 < \dots < \tilde{\lambda}_m < 1$. And let $\{(\tilde{\gamma}_i, \tilde{f}_i)\}_{i=1}^m$ be the first m eigenpairs of (1),

where $0 \leq \tilde{\gamma}_i < 1$. Then we have:

$$\begin{aligned} \tilde{\gamma}_i(2 - \tilde{\gamma}_i) &= \tilde{\lambda}_i, \\ \tilde{f}_i &= \begin{bmatrix} \tilde{t}_i \\ \tilde{z}_i \end{bmatrix}, \end{aligned}$$

where $\tilde{t}_i = \frac{1}{1-\tilde{\gamma}_i}P\tilde{z}_i$, and $P = D_c^{-1}\tilde{E}$ is the associated transition probability matrix from cells to representatives.

Let $\tilde{z}_1, \tilde{z}_2, \dots, \tilde{z}_m$ be the top m eigenvectors solution of the (2). $\tilde{t}_1, \dots, \tilde{t}_m$ is the top m eigenvectors of G_{xc} .

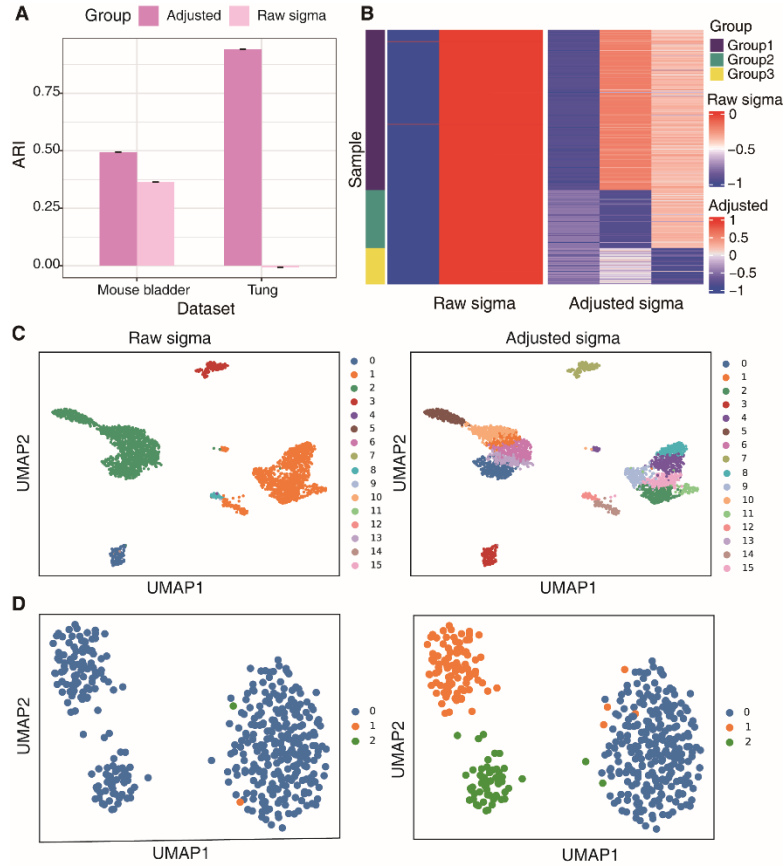


Fig. S1 Evaluation of scaled exponential similarity kernel function. **a**, The ARI of two datasets (Mouse Bladder and Tung) when used a traditional exponential similarity kernel (Raw sigma) that is the mean distance of all representatives and cells as well as scaled exponential similarity kernel (Adjusted). **b**, The heatmaps show the eigenvectors of the bipartite graph Laplacian on the tung dataset using the two different kernel function, where rows represent cells and columns represent the k first eigenvectors. The true labels are used as groups. **c**, **d**, The clustering distribution on the two datasets for the mouse bladder and tung datasets, respectively.

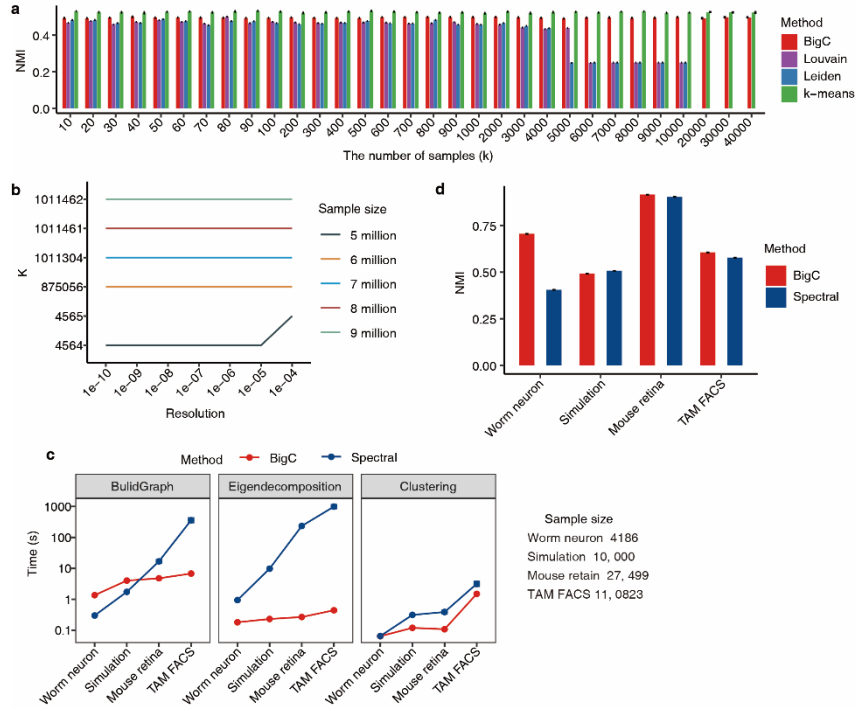


Fig. S2 Performance of BigC with other methods on simulation data and Comparison of consuming time with traditional spectral clustering. **a**, The NMI of different methods on simulation data with different sample sizes. **b**, Number of clusters estimated by Louvain for five simulated data with sample sizes ranging from 5 million to 9 million under different resolutions (x-axis). **c**, We divided the entire clustering to three steps and showed the time each step by our method and traditional spectral clustering on four datasets, including Mouse neuron, Simulation data, Mouse retina and TAM FACS with the cells ranging from 4,217 to 110,823, in which the number of sample size for the simulation data is 10 thousand. **d**, The NMI of two methods on these four datasets.

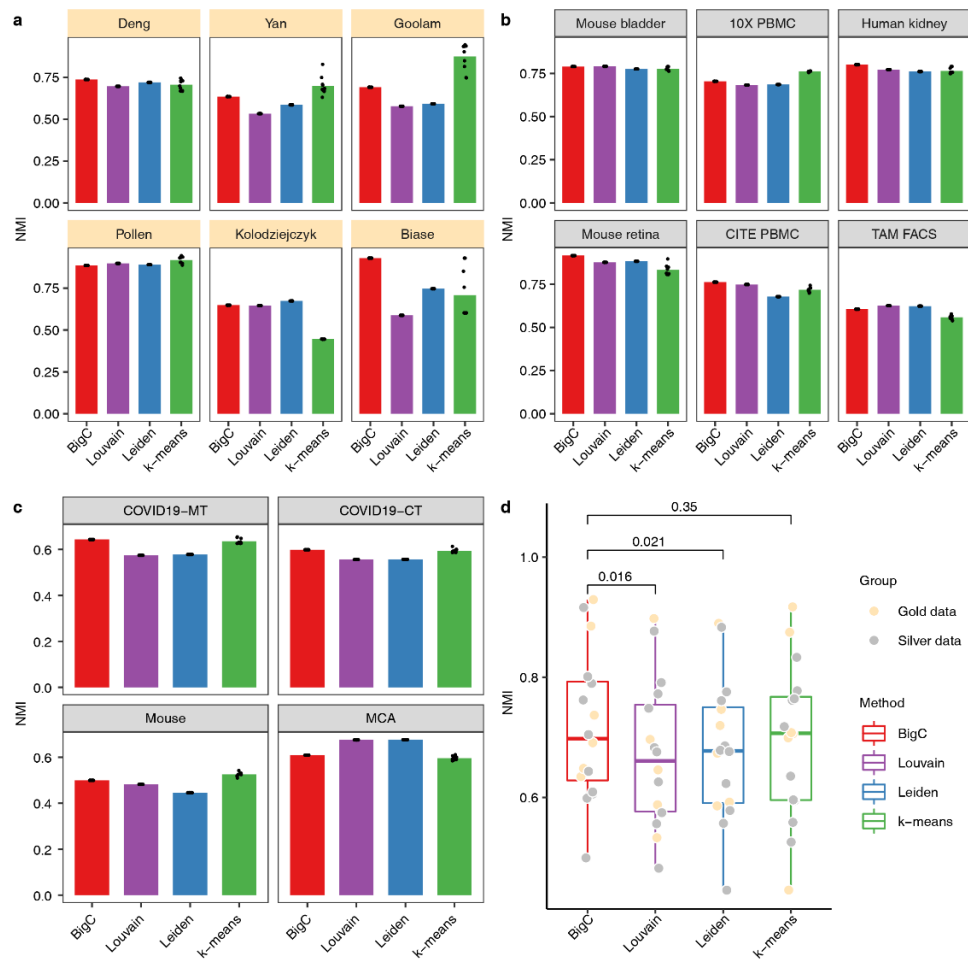


Fig. S3 The performance of four methods by NMI metrics on all 15 datasets. a-c, The NMI of six gold standard datasets (a), six silver datasets (b), and three large datasets (c). d, The overall NMI of four methods on 13 datasets.

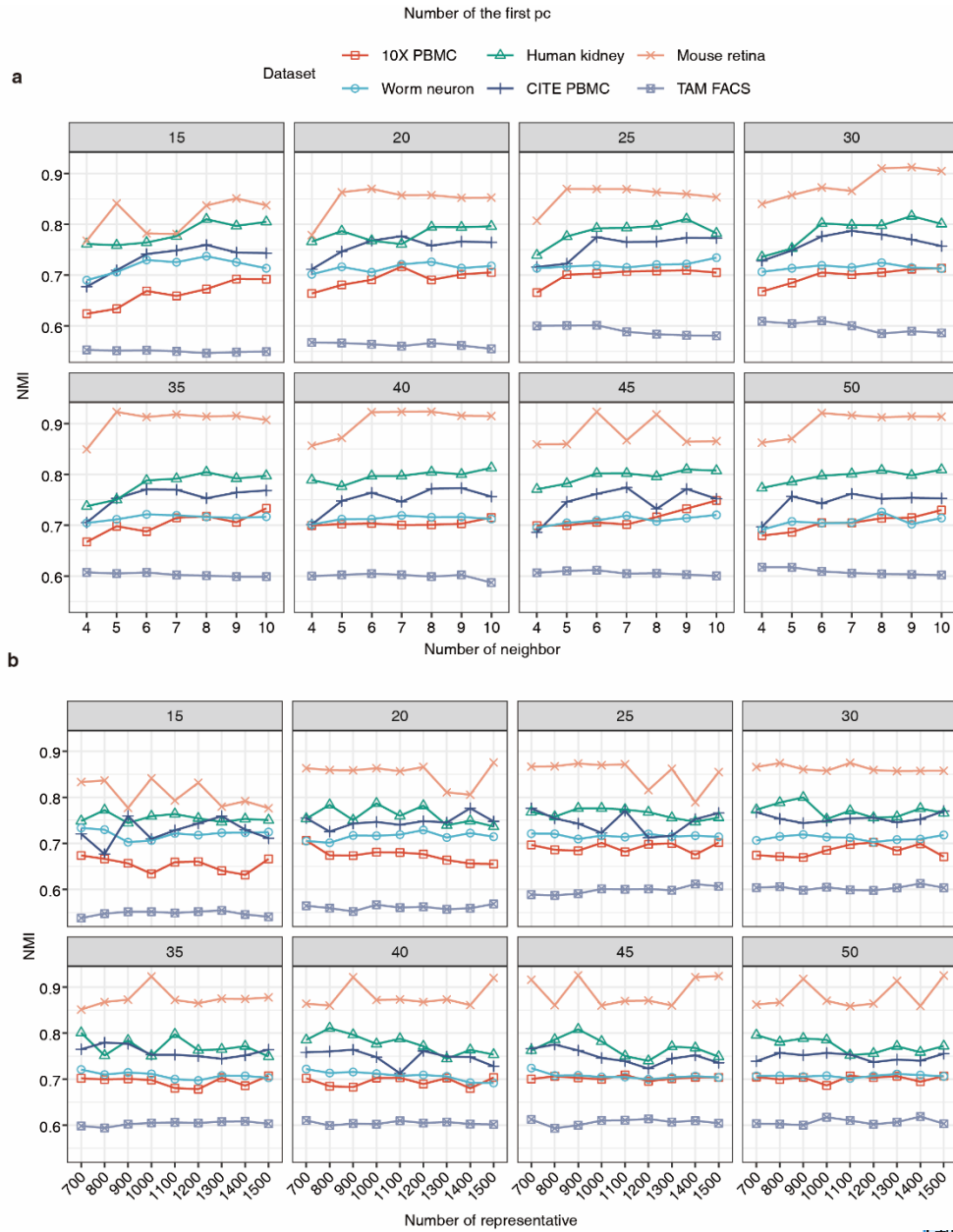


Fig. S4 The benchmark of parameters including number of principal components, representatives and number of k nearest neighbors. a, b, The clustering performance varies with (a) the number of principal components and (b) the number of neighbor representatives of each cell. Each panel plot represents the number of the principal components.

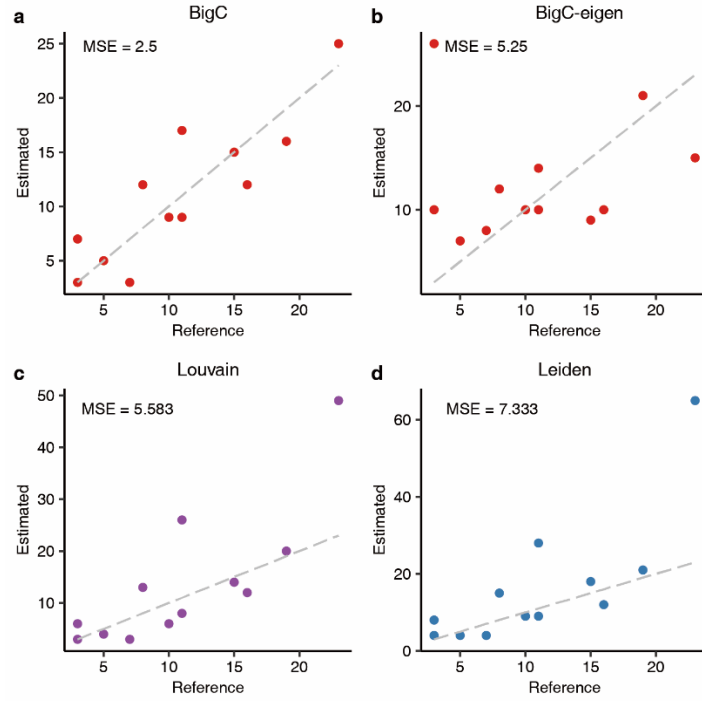


Fig. S5 The accuracy of the number of clusters estimated by different methods on twelve datasets. a-c, The correlation of estimated number clusters and reference labels across different methods, including Louvain (a), our methods eigenvalues-based (b) and community detection-based (c). We provide mean absolute error (MSE) for each. **d,** NMI of each method on all datasets, with the number of clusters by our method as input.

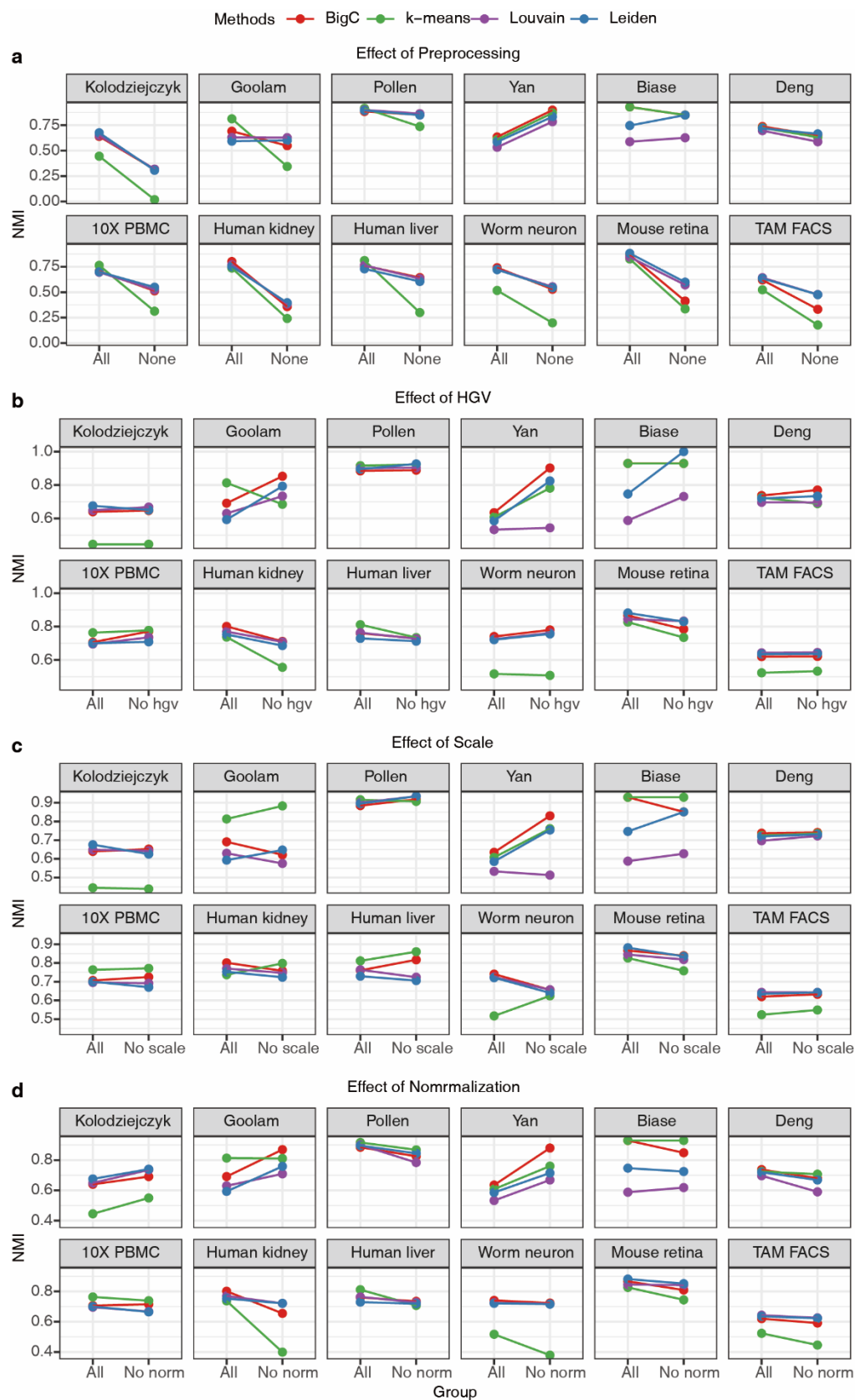


Fig. S6 The influence of data preprocessing approach on clustering results. a, The performance of clustering with and without preprocessing, in which "ALL" refers to four processing steps including normalization, logarithmic transformation, selection of high variable genes and scale (zero

mean and equal variance), and 'None' refers to remove this processing. Comparison of clustering accuracy between removing one of the steps and 'ALL', including removing normalization (**b**), logarithmic transformation (**c**), selection of high variable genes (**d**) and scale (**e**).

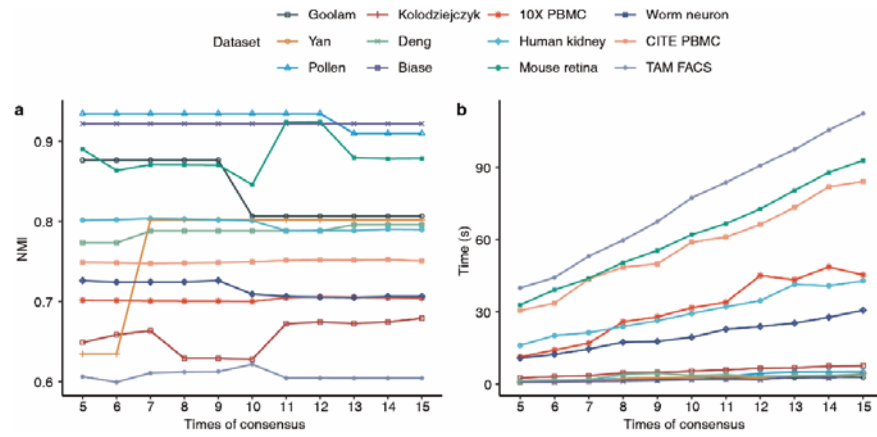


Fig. S7 Benchmark of consensus parameters of BigCC on twelve datasets. a, Clustering accuracy NMI varies as the number of consensus times increases. **b,** The relationship of consensus time and ensemble times on different datasets.